FOREX Publication
Open Access | Rapid and quality publishing

International Journal of
Electrical and Electronics Research (IJEER)
Research Article | Volume 12, Issue 2 | Pages 540-544 | e-ISSN: 2347-470X

Derivation of Generalized Design Formulas for Modified Branch-Line Coupler with the Second Harmonic Suppression Characteristics

In-Seon Kim[1], Hong-Kyun Ryu[2], Beom-Jun Park[3], Cheol-Soo Lee[4] and Joo-Rae Park[5*]

[1,2,3,4,5] *Agency for Defense Development, Daejeon, 34060, Korea Tel: 82-42-821-3545; Fax: 82-42-823-3400*

*Correspondence: *naechon199@naver.com*

ABSTRACT- We propose a modified branch-line coupler composed of the open stubs and stepped impedance lines. This structure allows the second harmonic suppression and size reduction. We present the steps to transform from a conventional branch-line coupler to the proposed structure using equivalent circuits and derive the generalized design formulas. From the results analysis of the design sample, we demonstrate the validity of the derived formulas. The fabricated branch-line coupler provides more than 30 dB the second harmonic suppression and about 30 % size reduction compared to a conventional branch-line coupler.

Keywords: equivalent circuit, stepped impedance line, design formulas, size reduction, harmonic suppression.

ARTICLE INFORMATION

Author(s): In-Seon Kim, Hong-Kyun Ryu, Beom-Jun Park, Cheol-Soo Lee and Joo-Rae Park;

Received: 03/01/2024; **Accepted**: 18/04/24; **Published**: 30/05/2024;
e-ISSN: 2347-470X;
Paper Id: IJEER 231039;
Citation: 10.37391/IJEER.120228
Webpage-link:
https://ijeer.forexjournal.co.in/archive/volume-12/ijeer-120228.html

crossref member
CROSSREF.ORG
THE CITATION LINKING BACKBONE

Publisher's Note: FOREX Publication stays neutral with regard to Jurisdictional claims in Published maps and institutional affiliations.

1. INTRODUCTION

Branch-line coupler (BLC) is important component that is widely applied in microwave circuit design such as power divider, combiner, mixer, antenna feeder, etc. A BLC has the advantages of obtaining a quadrature phase differences and -3dB coupling at output ports. However, a conventional branch-line coupler (CBLC) occupies a large surface area because it consists of four quarter wavelength transmission line. Due to this structure, miniaturization of the circuit is restricted. The restriction is more severe at low frequencies. In addition, the CBLC has harmonics occurred at the multiples of an operating frequency. Several studies have been conducted to overcome these drawbacks [1-15], Typically, there are two methods. The first method is to introduce slow-wave structure in the BLC [1-6]. The second method is to load the coupler with shunt stubs [7-15]. Most BLCs in these studies provide good size reduction and harmonic suppression properties. However, these studies often tend to depend on trial-and-error methods or empirical efforts to determine the dimension of BLCs due to the difficult of the design formulas and the complexity of the structures.

In this paper, we propose a modified BLC composed of four shunt open stubs and four stepped impedance lines (SILs). The proposed BLC (PBLC) has size reduction and the second harmonic suppression properties. We mainly focus on deriving the generalized design formulas that are readily available to anyone for PBLC design. As for size reduction and harmonic suppression, we only demonstrate the possibility and don't intentionally put much effort into them.

2. STRUCTURAL TRANSFORMATION USING EQUIVALENT CIRCUITS

We propose two steps to transform from CBLC to PBLC. The first step is to transform the transmission lines of the CBLC into equivalent structure consisting of π-type circuits and open stubs. The second step is to transform the π-type circuits into SILs [16,17]. Figure 1 is presented to explain the first step. Figure 1A shows a structure consisting of a CBLC and 8 shunt stub-sets. Here, one stub-set is configured as in Box B0. Figure 1A still has the general CBLC properties because the admittance sum of each stub-set is zero. The admittances Y_{p1} and Y_{p2} are arbitrarily chosen values. The lengths, θ_{p1} and θ_{p2}, are set to $\lambda_0/8$ at the center frequency (f_0) so that an attenuation pole capable of suppressing the second harmonic can be generated at $2f_0$.

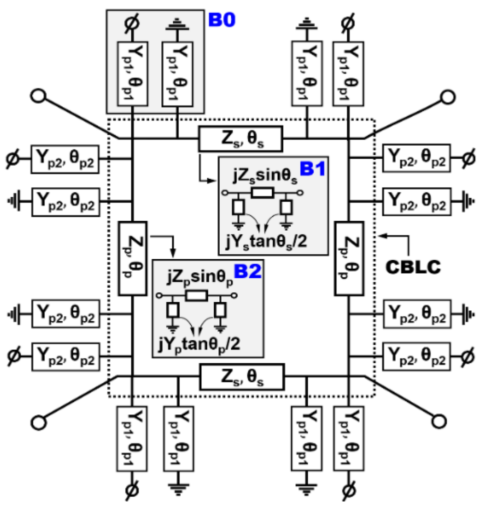

(A)

FOREX Publication
Open Access | Rapid and quality publishing
International Journal of
Electrical and Electronics Research (IJEER)
Research Article | Volume 12, Issue 2 | Pages 540-544 | e-ISSN: 2347-470X

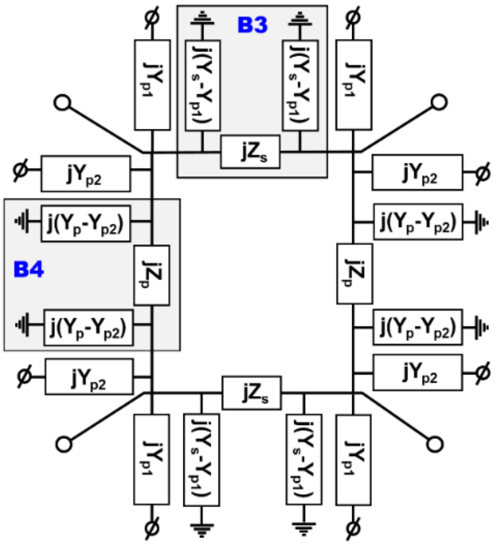

(B)

Figure 1 A, Configuration with shunt open stubs sets added to CBLC; B, Transformation using π-type equivalent circuit.

In *figure 1(A)*, if transmission lines of a CBLC are transformed to π-type equivalents, they are transformed into boxes B1 and B2. The impedances, Z_s and Z_p, are 35.35Ω and 50Ω, respectively. The *figure 1(A)* is transformed to *figure 1B* by the sum of the shunt elements in box B1 and the short stub in box B0. The following process is the second step of transforming boxes B3 and B4 in *Figure 1(B)* into boxes B6 and B8 in *figure 2*, respectively. *Figure 2* shows the final structure proposed in this paper.

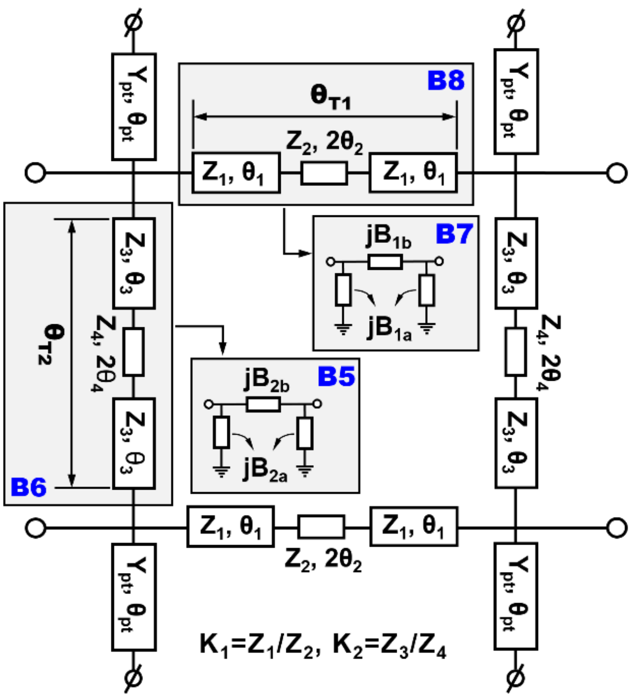

Figure 2. Transformation from π-type circuit to SIL structure.

In *figure 2*, in order to reduce the complexity of calculating trigonometric function, the middle line length of SIL is defined as $2\theta_{2\,(\text{or } 4)}$. K_1 and K_2 are defined as the impedance ratios of the transmission lines constituting the SILs. Z_1, Z_2, Z_3, and Z_4 are arbitrarily chosen values. IF the boxes B7 and B8 are equivalent circuits, the susceptances in box B7 can be obtained by the even and odd mode method as follows.

$$B_{1a} = \frac{Y_1[K_1 tan(\theta_2) + tan(\theta_1)]}{1 - K_1 tan(\theta_2) tan(\theta_1)} \quad (1)$$

$$B_{1b} = \frac{1}{2} \cdot \frac{Y_1[tan(\theta_1) - K_1 cot(\theta_2)]}{1 + K_1 cot(\theta_2) tan(\theta_1)} - \frac{1}{2} \cdot B_{1a} \quad (2)$$

IF box B3 in Figure 1B and box B7 in Figure 2 are equivalent circuits, B_{1a} and B_{1b} can also be expressed as Equation (3) and (4), respectively.

$$B_{1a} = Y_s - Y_{p1} \quad (3)$$

$$B_{1b} = -Y_s \quad (4)$$

Since Equation (1) and Equation (3) are the same, the following equation can be obtained.

$$tan(\theta_2) = \frac{[Y_s - Y_{p1} - Y_1 tan(\theta_1)]}{K_1[Y_1 + (Y_s - Y_{p1}) tan(\theta_1)]} \quad (5)$$

Applying *equation (5)* to *equation (1)* and using the condition that *equation (2)* and *equation (4)* are the same, θ_1 can be obtained as *equation (6).*

$$\theta_1 = tan^{-1}\left(\frac{-A_2 + \sqrt{A_2^2 - 4A_1A_3}}{2A_1}\right) \quad (6)$$

Where A_1, A_2, and A_3 are as follows:

$$A_1 = Y_1^2[K_1^2(Y_{p1}^2 - Y_s^2) + Y_1^2]$$

$$A_2 = -2Y_1^3 Y_{p1}(K_1^2 - 1)$$

$$A_3 = Y_1^2(Y_{p1}^2 - Y_s^2 + K_1^2 Y_1^2)$$

Then, by substituting *equation (6)* into *equation (5)*, θ_2 can be obtained as *equation (7)*

$$\theta_2 = tan^{-1}\left(\frac{[Y_s - Y_{p1} - Y_1 tan(\theta_1)]}{K_1[Y_1 + (Y_s - Y_{p1}) tan(\theta_1)]}\right) \quad (7)$$

In the same way as before, if boxes B4, B5 and B6 are equivalent, θ_3 and θ_4 are obtained in *equations (8) and (9)*, respectively.

$$\theta_3 = tan^{-1}\left(\frac{-B_2 + \sqrt{B_2^2 - 4B_1B_3}}{2B_1}\right) \quad (8)$$

Where B_1, B_2, and B_3 are as follows.

$$B_1 = Y_3^2[K_2^2(Y_{p2}^2 - Y_p^2) + Y_3^2]$$

$$B_2 = -2Y_3^3 Y_{p2}(K_2^2 - 1)$$

$$B_3 = Y_3^2\left(Y_{p2}^2 - Y_p^2 + K_2^2 Y_3^2\right)$$

$$\theta_4 = tan^{-1}\left(\frac{[Y_p - Y_{p2} - Y_3 tan(\theta_3)]}{K_2[Y_3 + (Y_p - Y_{p2})tan(\theta_3)]}\right) \quad (9)$$

The admittance (Y_{pt}) of the open stub in *figure 2* is obtained by summing the admittances of the adjacent open stubs at each node in *figure 1(B).*

$$Y_{pt} = Y_{p1} + Y_{p2} \quad (10)$$

The length of the open stub, θ_{pt}, is as follows.

$$\theta_{pt} = \theta_{p1\,(or\,p2)} \quad (11)$$

Here, θ_{pt} is set to $\lambda_0/8$ at the center frequency. All variables in *equations (6) – (11)* are known values. Accordingly, we can calculate all the design parameters required for PBLC design using the Equations derived above.

On the other hand, we examined how the impedance ratio of the SIL and the impedance of the open stub affect the total length of the SIL. *Figure 3* shows the change in $\theta_{T1(or\ T2)}$ according to $K_{1(or\ 2)}$ and $Z_{p1(or\ p2)}$.

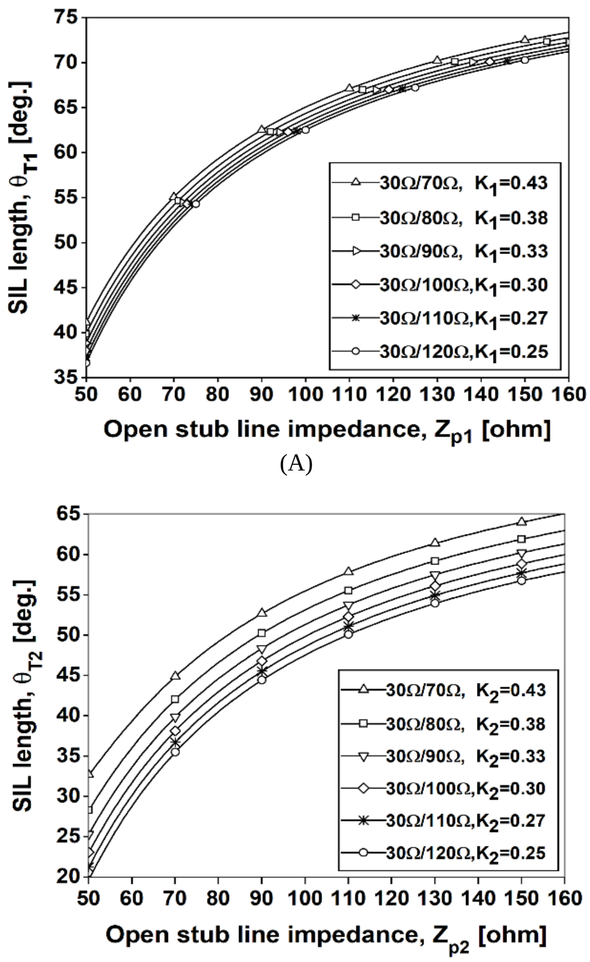

(A)

(B)

Figure 3 A, Open stub impedance vs. total length of the horizontal SIL for each K1; B, Open stub impedance vs. total length of the vertical SIL for each K2.

In *figure 3*, we can confirm that not only the impedance ratio of SIL but also the open stub impedance is important variable for changing the total length of the SIL. it can also be seen that the smaller open stub impedance and the smaller the impedance ratio, the shorter the SIL length. Therefore, these properties are properly applied to the PBLC design, it is expected to greatly contribute to size reduction. *Table 1* shows a list of SIL lengths and relative area compared to the CBLC for several cases in *figure 3.*

Table 1 Comparison of relative area

K_1 or K_2 ($Z_{1(or\ 3)}$ /$Z_{2(or\ 4)}$)	Z_{p1} or Z_{p2} [Ω]	θ_{T1} ([°]/[λ_0])	θ_{T2} ([°] / [λ_0])	$\theta_{T1}\times\theta_{T2}$ [λ_0^2]	Relative area [%]
0.43	70	55.05/0.53	44.89/0.125	0.0191	30.6
(30Ω/70Ω)	80	58.27/0.162	49.24/0.137	0.0222	35.5
0.33	70	39.88/0.111	53.44/0.148	0.0164	26.2
(30Ω /90Ω)	80	57.82/0.161	44.64/0.124	0.0200	32.0
0.25	70	51.85/0.144	35.50/0.098	0.0141	22.6
(30Ω/120Ω)	80	56.38/0.157	40.53/0.113	0.0177	28.3

As we can see in *figure 3* and *table 1*, it is theoretically possible to reduce the rectangular area composed of SILs by more than 70% compared to the area of the CBLC. However, the size reduction of the PBLC is restricted by the length of the open stubs. In order to mitigate this restriction, if shunt elements are optimally arranged in the inner space between the SILs.[2-6], it is expected that the size of the PBLC can be significantly reduced.

3. SIMULATION AND MEASUREME-NT

To demonstrate the validity of the PBLC design equations derived above, we designed a PBLC with f_0 = 2 GHz, Z_{p1} = Z_{p2} =160 Ω, Z_1 = Z_3 =30 Ω, Z_2 = Z_4 =80 Ω, Z_s = 35.35 Ω, Z_p = 50 Ω, and θ_{p1} = θ_{p2} = 45°. θ_1, $2\theta_2$, θ_3, and $2\theta_4$ calculated using *equations (5) – (8)* are 31.72°, 9.32°, 16.8°, and 29.42°, respectively. Z_{pt} is calculated as 80 Ω by *equations (10).* The simulation was performed for a microstrip structure of the substrate with ε_r = 2.2, h = 0.7874 mm, and tan δ = 0.0004. We used ANSYS's HFSS as simulation tool. Figure 4 shows the EM simulation results of PBLC (solid lines) and CBLC (dotted lines). Return losses, S11, S22 and S33, are identical due to the symmetric structure of PBLC. Therefore, we show only S11 in *figure 4.*

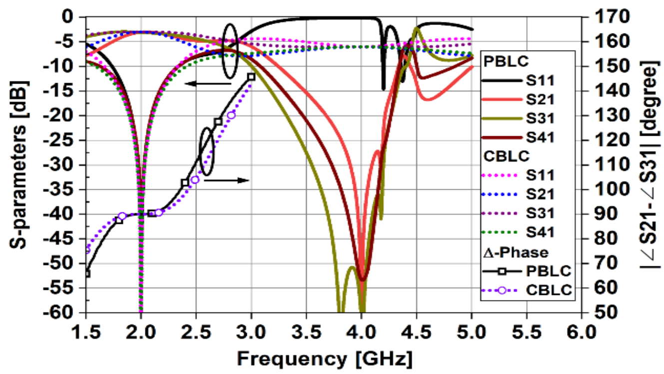

Figure 4. The simulation results of CBLC and PBLC

Research Article | Volume 12, Issue 2 | Pages 540-544 | e-ISSN: 2347-470X

In *figure 4*, the passband characteristics of PBLC and CBLC are very similar, but the biggest difference is that PBLC, unlike CBLC, has attenuation poles at the second harmonic frequency as originally intended. Based on the simulation result, a PBLC as shown in *figure 5* was fabricated.

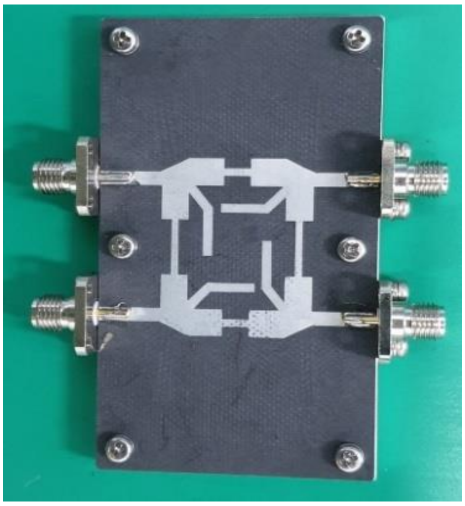

Figure 5. Photograph of the fabricated PBLC.

The dimension of PBLC excluding transmission lines for ports was measured as 23.22 mm × 29.34 mm. The dimension of CBLC was 29.34 mm × 33.16 mm. Therefore, the PBLC is about 30 % size smaller than CBLC. As mentioned above, this size reduction is only a design sample. In *figure 5*, It can be seen that the size of the PBLC can be reduced even more with only a dense arrangement of open stubs because there is still sufficient margin in the inner space between the SILs. *Figure 6* describes the measured results. It was observed that the measured result has a slight difference from the simulation result in *figure 4*. We believed that these differences were caused by inaccurate PCB etching, tuning process, and measurement without housing. Even if there are some deviations, the overall performances are very similar compared to simulation results.

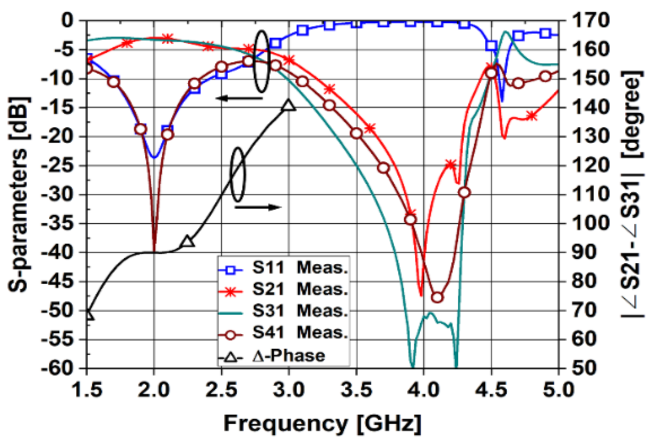

Figure 6. Measured results.

The passband return loss and insertion loss were measured to be more than 20 dB and less than 0.12 dB, respectively. The attenuation level at $2f_0$ is about –40 dB. In addition, the phase difference between ports at the center frequency is exactly 90 degrees. More detailed results are described in *table 2*. In addition, *table 2* compares representative characteristics of simulation and measured results. Here, we can clearly demonstrate that the agreement with simulation and measured results.

Table 2 Summary of simulation and measured results

	S-Para.	RL [dB] (at f_0)	IL [dB] (at f_0)	Att. Level [dB] (at $2f_0$)	Frac. BW [%] (> -3±0.5 dB)	Isolation [dB] (at f_0 / $2f_0$)	Freq. range [GHz] |∠S21-∠S31| (> 90±1°)
Sim.	S11	< 30	-	-	-	-	1.92 ~ 2.15
	S21		2.98	< 30	16.5	-	
	S31		3.28	< 50	31.8	-	
	S41		-	-	-	< 30 / < 50	-
Meas.	S11	< 22	-	-	-	-	1.85 ~ 2.21
	S21		3.07	< 30	18.2	-	
	S31		3.11	< 50	36.1	-	
	S41		-	-	-	< 30 / < 50	-

By summarizing the above results, we finally confirmed the validity of the derived design formulas and that the PBLC structure is suitable for size reduction and the second harmonic suppression. *Table 3* shows the performance comparison of the proposed design with several previous designs.

Table 3 Comparison with previous reported BLCs

Ref.	Freq. (GHz)	First Harmonic suppression	Presenting Design Formulas	Configuration elements
[7]	0.93	$3f_0$	No	4 uniform lines, 4 radial stubs
[8]	1	$2f_0$	No	4 uniform lines, 8 open stubs
[9]	1	$4f_0$	Yes	4 step impedance lines
[10]	2.4	No	No	4 step imps. lines, 4 stepped imp. open stubs
[11]	1	$3f_0$	No	4 uniform lines, 8 stepped imp. open stubs
This work	2	$2f_0$	Yes	4 step imp. lines, 4 open stubs

Except for [9], the comparative papers do not present design formulas. Therefore, repeated efforts are required to design BLCs. Meanwhile, when the BLC in [9] is used with active devices, it is difficult to suppress the intermodulation products near the passband because the first attenuation pole is formed at the third harmonic. On the other hand, the proposed BLC provides second harmonic suppression and generalized design formulas. These are the main advantages of our BLC.

5. CONCLUSION

We proposed a simple BLC structure capable of harmonic suppression and size reduction, and derived generalized design formulas that allow us to obtain all design variables of the proposed structure. Through a series of processes, including design, simulation, fabrication, and measurement, we confirmed that the design formulas were accurately derived. The fabricated PBLC has the second harmonic suppression performance of 40 dB or more. We did not put much effort into size reduction because the derivation of the design formulas was the main focus of our study. Nevertheless, the size has been reduced by about 30% compared to CBLC. This size reduction is only applicable to the design sample in this paper. We expect to achieve a size reduction ratio greater than the current level by implementing short SILs with appropriate selection of design parameters and efficiently arranging shunt stubs in inner space between the SILs.

ACKNOWLEGMENT

This work was supported by the Agency for Defence Development Grant funded by the Korean Government (912971201).

REFERENCES

[1] J. Selga, P. Velez, J. Comina, A. Fenandez-Prieto et al., “Harmonic suppression in branch-line coupler based on slow-wave transmission lines with simultaneous inductive and capacitive loading,” Microwave and Optical Technology Letters, vol. 60, iss. 10, pp. 2374-2384, Oct 2018.

[2] J. Selga, J. Coromina, P. Velez, A. Fenandez-Prieto et al., “Miniaturized and harmonic-suppressed rat-race coupler based on slow-wave transmission lines,” IET Journal, vol. 13, iss. 9, pp. 1293-1299, July 2019

[3] Youngqiang Wang, Jaixue Ma, “A Compact Branch-Line Using Substrate Integrated Suspended Line Technology,” IEEE Microwave and Wireless Components Letters, vol. 26, iss. 2, pp. 95-97, Feb 2016.

[4] J. Coromina, J. Selga, P. Velez, J. Bonache, and F. Martin, “Size reduction and harmonic suppression in branch line couplers implemented by means of capacitively loaded slow-wave transmission lines,” Microwave and Optical Technology Letters, vol.59, iss. 11, pp. 2822-2830, Nov 2017.

[5] Z. Zhao, S. Wang, X. Chen et al., “Miniaturized Microstrip Branch-line Coupler with Wideband Harmonic suppression Using Modified Radial Stub Loaded Resonators,” in 2023 15th International Conference on Communication Software and Network Chana-Japan Joint Microwave Conference, Shenyang, China, 2023, pp. 21-23.

[6] Saeed. Roshani, Salah I. Yahya, Sobhan Roshani et al., “Design of a Modified Compact Coupler with Unwanted Harmonics Suppression for L-Band Applications,” electronics, vol. 11, iss. 11, pp. 1747-1762, May 2022.

[7] A. R. Hazeri, A. Kashaninia, T. Faraji, and M. F. Arani, “Miniaturization and harmonic suppression of the branch-line coupler based on radial stubs,” IEICE Electronics Express, vol. 8, iss. 10, pp. 736–741, Aug 2011.

[8] H. Cui, J. Wang and J. L. Li, “Compact Microstrip Branch-line Coupler with Wideband Harmonic Suppression,” ACES Journal, vol. 27, iss. 9, pp. 766-771, Sep 2012.

[9] S. H. Sedighy and M. Khalaj-Amirhosseini, “Compact Branch-line Coupler using Step Impedance Transmission Lines (SITLs),” ACES Journal, Vol. 28, iss. 9, pp. 866-870. Sep 2013.

[10] Sh. Nouri, J. Nourinia, N. Valizade, B. Mohammadi, and A. Valizade, “Novel Compact Branch-Line Coupler Using Non-Uniform Folded Transmission Line and Shunt Step Impedance Stub with Harmonics Suppression,” ACES Journal, vol. 31, iss. 4, pp. 401-409. Apr 2016.

[11] J. Coromina, P. Velez, J. Bonache, and F. Martin, “Branch Line Coupler with Small Size and Harmonic Suppression Based on Non-Periodic Step Impedance Shunt Stub (SISS) Loaded Lines,” IEEE Access, vol. 8, pp. 67310-67320, Apr 2020.

[12] V. Krishna Velidi and A. Bhattacharya, “A Stub Tapped Compact Hybrid Coupler with Broad-Band Harmonic Rejection,” in TENCON 2008- 2008 IEEE Region 10 Conference, Hyderabad, India, 2008, pp. 19-21.

[13] Z. B. Khan, G. Mehdi, and H. Zhao, “Design of a Compact Hybrid Branch Line Coupler with 2-D Implementation of Stepped Impedance Transmission Lines of High Impedance Ratio for Wide Range of Harmonic Suppression,” ACES Journal, vol. 34, iss. 8, pp. 1211-1218. Aug 2019.

[14] V. K. Velidim and A. Bhattacharya, “Miniaturized Planar 90° Hybrid Coupler with Unchanged Bandwidth Using Single Characteristic Impedance Line,” in Chana-Japan Joint Microwave Conference, Shanghai, China, 2008, pp. 10-12.

[15] I. S. Satya and S. Mukherjee, “Compact Substrate Integrated Coaxial Line Quadrature Hybrid with Harmonic Rejection,” in IEEE Asia-Pacific Microwave Conference (APMC), Singapore, 2019, pp. 10–13.

[16] M. Sagawa, M. Makimoto, and S. Yamashita, “Geometrical Structure and Fundamental Characteristics of Microwave Stepped-Impedance Resonator,” IEEE Transactions on Microwave Theory Techniques, vol. 45, iss. 7, pp. 1078-1085, July1997.

[17] I. S. Kim, C. H Lee, and Dal Ahn, “A Smaller Step Impedance Line Wilkinson Power Divider with an Improved Better Stop-Band,” Microwave and Optical Technology Letters, vol. 58, iss. 7, pp. 1607-1610, July 2016.